

Evidence for Fully Conjugated Double-Stranded Cycles

Malte Standera,^[a] Rolf Häfliger,^[b] Renana Gershoni-Poranne,^[c] Amnon Stanger,^[c] Gunnar Jeschke,^[d] Jacco D. van Beek,^[e] Louis Bertschi,^[b] and A. Dieter Schlüter*^[a]

Abstract: A chain of circumstantial evidence for the existence of the first fully conjugated, double-stranded cycles is presented. The products have the structure of the belt-region of fullerene C₈₄ (D₂) and carry either four hexyl chains or four phenyl groups. The unsubstituted parent cycle is also presented. The chain of evidence is mainly based on mass spectrometric analysis and trap-

ping reactions, the latter being supported by quantum mechanical calculations. It is also of importance that the phenyl-substituted and unsubstituted products cannot undergo a [1,5] hydro-

Keywords: aromaticity · conjugation · mass spectrometry · thermochemistry · trapping experiments

gen shift, the only reasonable side-reaction that recently could not be excluded for the alkyl-substituted analogue. It is concluded that the fully aromatic targets truly exist in the gas phase. Whether they can be generated in solution under the applied conditions cannot yet be firmly decided; theoretical evidence speaks against.

Introduction

Chemists have dreamed of fully unsaturated, double-stranded hydrocarbon cycles like *[n]*cyclacenes **I**, buckybelts **II**, cyclo*[n]*phenacenes **III**, and Vögtle-belts **IV** for several decades (Figure 1).^[1] In addition to their aesthetic appeal, they are also important for the study of certain aspects of host-guest behavior, including hydrogen bonding between weak donors and π systems, the formation of polyrotaxanes, the *endo/exo* cyclic selectivity of reactions, the dynamics of transition-metal fragments complexed to the π system, and their

redox behavior, including the aspect of maximum chargeability. They would also serve as models for their open-chain linear analogues, the ladder polymers,^[2] and some of them could be developed into novel, shape-persistent constituents for molecular constructions.^[3] Finally, such compounds would enrich the world of larger, all-carbon structures such as fullerenes, carbon nanotubes, and graphene. Although there has been significant progress in their synthesis, a breakthrough has not yet been achieved. Several double-stranded cycles with the appropriate carbon skeletons have been synthesized and even a few chemical modifications aimed at an expansion of the conjugated parts have been accomplished.^[4] However, attempts to generate any of the above fully conjugated targets failed altogether and only recently has synthesis gotten close, specifically the work of

- [a] Dr. M. Standera, Prof. A. D. Schlüter
Laboratory of Polymer Chemistry
Department of Materials, ETH Zürich
Wolfgang-Pauli-Strasse 10, HCI 541, 8093 Zürich (Switzerland)
E-mail: dieter.schluter@mat.ethz.ch
- [b] R. Häfliger, L. Bertschi
Mass Spectrometry Unit, Laboratory of Organic Chemistry
Department of Chemistry and Applied Biological Sciences
ETH Zürich
Wolfgang-Pauli-Strasse 10, 8093 Zürich (Switzerland)
- [c] R. Gershoni-Poranne, Prof. A. Stanger
Schulich Faculty of Chemistry and
The Lise-Meitner-Minerva Center for
Computational Quantum Chemistry, Technion
Technion City, 32000 Haifa (Israel)
- [d] Prof. G. Jeschke
Laboratory of Physical Chemistry, ETH Zürich
Wolfgang-Pauli-Strasse 10, HCI F 231, 8093 Zürich (Switzerland)
- [e] Dr. J. D. van Beek
Laboratory of Solid-State NMR Spectroscopy
Department of Chemistry and Applied Biological Sciences
ETH Zürich
Wolfgang-Pauli-Strasse 10, 8093 Zürich (Switzerland)

Supporting information for this article is available on the WWW under <http://dx.doi.org/10.1002/chem.201100443>.

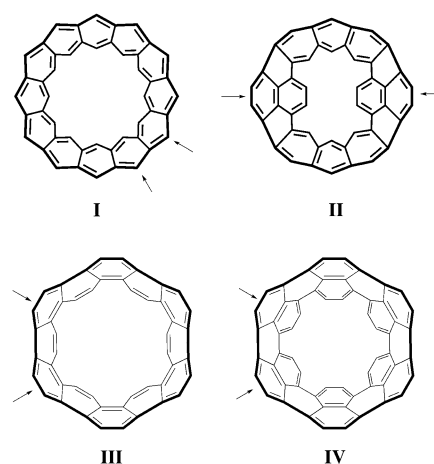


Figure 1. Fully conjugated, belt-like compounds, *[n]*cyclacenes **I** ($n=12$) and buckybelts **II** (shown with two repeat units), and angularly annulated congeners, the cyclo*[n]*phenacenes **III** ($n=12$) and the Vögtle belts **IV** (shown with six repeat units). The arrows help identify the repeat units.

Bodwell,^[5] Iyoda,^[6] and ourselves.^[7] The reasons for this considerable complication are target specific, but, by and large, also have something to do with the curvature of the compounds, rendering a fully conjugated structure energetically less favorable than noncurved, flat analogues. This energy cost makes the final “aromatization” step more complicated to achieve and also the target structure, once accomplished, more prone to subsequent reactions, which may go as far as to render it transient and nonisolable.

Our laboratory recently provided high-resolution mass spectrometric evidence for a compound with the same molar mass as **4a** (Figure 2), a tetrahexyl-substituted bucky-belt derivative of type **II**.^[7a] The product was obtained by thermolysis of the tetraacetate **3a** at 330 °C. Although this precursor has the same carbon skeleton as **4a**, it cannot be excluded that, instead of **4a**, a rearranged isomer was analyzed. This isomer may have formed either by passing through the intermediate **4a** or by surpassing it. Unfortunately, neither the relatively drastic reaction conditions nor the energetic considerations based on computations^[7a] allowed this possibility to be excluded. In particular, isomers of **4a** resulting from [1,5] hydrogen shifts^[8] seemed possible. We therefore initiated a broader study into this matter that comprised 1) completion of the experiments based on the hexyl system and 2) usage of precursors with the same carbon skeleton as target **II** but with lateral substituents that would render a hydrogen shift impossible (Ph and H instead of C₆H₁₃). The relevant compounds are presented in Figure 2. In particular, for the laterally unsubstituted compounds (**1c–4c**), serious solubility issues had to be expected. In light of the importance of the goal of this work, this drawback was nevertheless accepted. Herein we report on the outcome of this broader study, aimed at the three target

compounds **4a–c**. It comprises optimizations and novel syntheses, trapping reactions supported by quantum-chemical calculations as well as NMR, EPR, and UV spectroscopic and mass spectrometric investigations. As will be shown, none of the evidence provided represents stand-alone unequivocal proof. The combination of the results obtained, however, condenses into a rather conclusive picture that suggests the existence of fully conjugated, double-stranded cycles of type **II**.

Results

All the compounds shown in Figure 2 were synthesized according to the published procedure based on the hexyl system.^[7] For this reason, the syntheses will not be described in the main text, and the reader is referred to the Supporting Information, which provides the relevant schemes, procedures, and analytical data in detail. The tetrahydrate **1a**^[7a] was prepared on a several-gram scale and its acid-catalyzed dehydration gave **2a**, as is already known. The new tetrahydrate **1b** was synthesized on a smaller scale and analyzed by spectroscopic and spectrometric means only. The corresponding **1c** was not isolated but rather analyzed directly from the crude product mixture by mass spectrometry only.

The following aspects were investigated and will be reported below:

- 1) The thermolysis of **3a** with specific focus on procedural optimizations and trapping of the presumed target **4a** by Diels–Alder dienophiles.
- 2) Computational studies on the expected products of these trapping reactions with the aim of estimating their exothermicity and obtaining the corresponding adduct structures.
- 3) The attempted generation of **4b** from **1b** as well as from **3b** and of **4c** from **3c**.
- 4) The formation of radical species under the conditions of thermolysis and dehydration.
- 5) The attempted purification, revealing the transient nature of the thermolysis products.

Thermolysis of tetraacetate **3a** and trapping experiments:

Until now, the thermolysis of **3a** was performed in a metal bath preheated to 330 °C for 3 min under vacuum and in the presence of a large excess (approximately 10-fold by mass) of parent anthracene. In this work, factors such as vacuum, temperature, time, and additives (e.g., solvents, acid quenchers, and trapping agents) were varied. A detailed description is available in ref. [9]. The optimum conditions were concluded to be 330 °C, 5 min, an excess of sodium carbonate, a nitrogen atmosphere at ambient pressure, and 1,10-phenanthroline as both solvent and Diels–Alder trapping agent. These conditions resulted in higher reproducibility and a cleaner reaction course. For example, the products obtained from a 3 or 5 min thermolysis were practically identical.

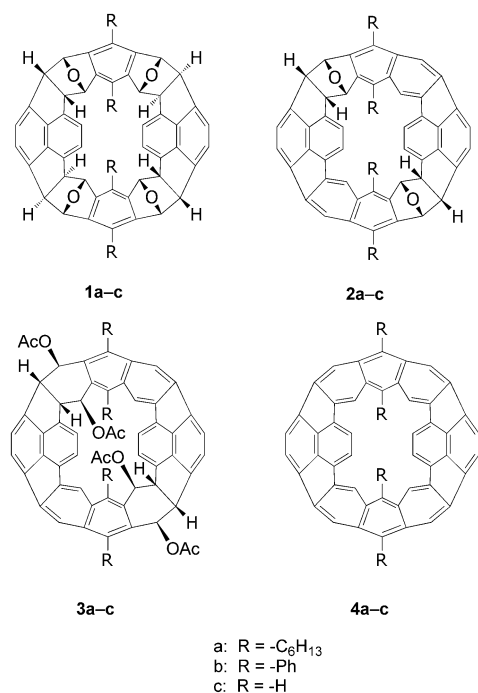


Figure 2. Compounds **1a,b,c–4a,b,c** of relevance in this study.

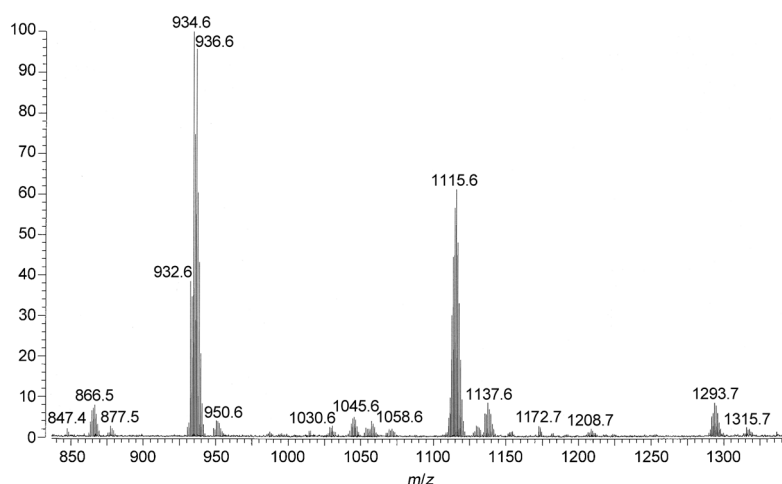


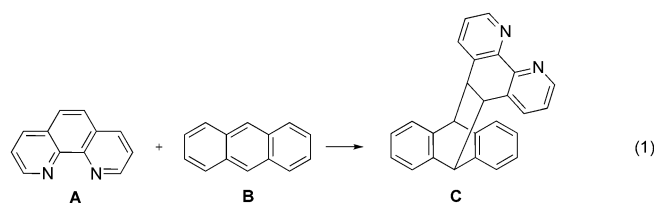
Figure 3. MALDI-FT mass spectrum of the crude mixture resulting from the thermolysis of **3a** in the presence of 1,10-phenanthroline showing the known isotopic patterns at m/z 932 [M]⁺, 934 [$M+2H$]⁺, and 936 [$M+4H$]⁺ and the signal groups centered at m/z 1116 [$M+\text{phen}$]⁺ and 1294 [$M+2\text{phen}$]⁺.

Figure 3 shows a typical and representative MALDI-FT mass spectrum of the crude product obtained from thermolysis under such conditions. In contrast to the previous conditions, in which anthracene was used as a solvent, no signals were observed that stem from cycles still containing acetate functions. Thus, the conversion under the optimized conditions was clearly higher. In addition to the signal group at m/z 932 [M]⁺, 934 [$M+2H$]⁺, and 936 [$M+4H$]⁺, the spectrum shows relatively complex signal groups centered at m/z 1116 and 1294, with the latter being somewhat simpler. The masses of these two groups correspond to protonated and nonprotonated mono- and diphenanthroline adducts of the compounds with m/z 932 and 934.^[10] If 2,9-dimethyl-1,10-phenanthroline was used instead, the corresponding mono- and diadducts were observed at m/z 1144 [$M+\text{phen}$]⁺ and 1350 [$M+2\text{phen}$]⁺. If this trapping agent was replaced by 4,4'-dimethyl-2,2'-bipyridyl, which lacks a dienophile, no adduct was detected. This suggests that Diels–Alder addition reactions take place with the phenanthrolines,^[11] however, firm structural conclusions cannot be drawn. Note that the observed adducts did not form in the mass spectrometer but rather during thermolysis. This was confirmed by recording a mass spectrum of a blend consisting of a sample prepared from a thermolysis product generated in the absence of a trapping agent and 2,9-dimethyl-1,10-phenanthroline. This spectrum did not show any indication of adducts. Finally, note that on the basis of ball-and-stick model considerations, a host–guest complex formed between the presumed fully conjugated target **4a** and the “trapping” agents could not have formed and thus cannot explain the signal at m/z 1116. There is a final aspect relating to the mass spectrum shown in Figure 3 that is worth mentioning. This regards the low intensity signals at m/z 950, 1138, and 1316. In the hundreds of mass spectra recorded of the thermolysis products, these signal groups appeared in each experiment. Their intensity depended upon reaction time and the amount of carbonate present. For long times (longer than 10 min) and

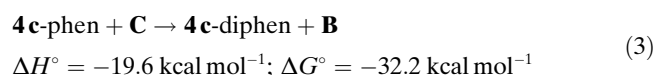
high amounts of carbonate, the intensity increased. Whether these signals are due to the presence of an oxygen atom in the cycle or a “water” molecule could not be clarified with certainty. Also, it could not be clarified whether this increased mass is due to residual fragments or due to addition reactions, the latter considered to be the more likely case. Similar effects have been reported previously.^[12]

Computational studies: The enthalpy and free energy of the trapping reactions were calculated by the following approach: The model reaction [reaction (1)] of addition of phenanthroline (**A**) to anthracene (**B**) was calculated at the G3

level of theory to obtain reliable thermochemical data. The thermochemistry of the addition of one and two phenanthroline molecules to **4c** was estimated by using isodesmic reactions, the energies of which were obtained at the B3LYP/6-311G* level of theory. Isodesmic reactions are much less sensitive to the computational level and therefore their results can be considered accurate. The DA reaction of **A** and **B** is endothermic by 2.3 kcal mol⁻¹ (at the G3 level).



Reactions (2) and (3) compare the addition of phenanthroline to **4c**, this unsubstituted compound serving as a model for **4a**. These reactions are highly exothermic: -15.3 kcal mol⁻¹ for the first addition and -19.6 kcal mol⁻¹ for the second. Considering reaction (1), this means that the addition of the first and second phenanthroline molecules to **4c** are exothermic by 13.0 and 17.3 kcal mol⁻¹, respectively.



As in other reactions of **4**,^[7a] these results can be explained by the release of strain following the DA reactions (Figure 4).

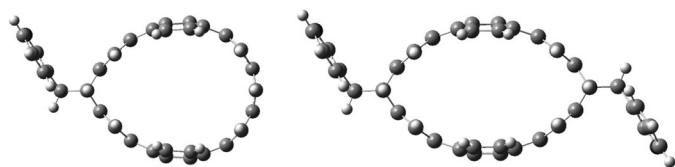


Figure 4. Calculated structures of compounds “4c-phen” (left) and “4c-diphen” (right), the products of a DA trapping reaction involving the central ring of the anthracenes of **4c**.

Interestingly, the ΔG° values for reactions (2) and (3) are -28.7 and -32.2 kcal mol $^{-1}$, respectively. Unlike the comparison between hydrated anthracenes and hydrated cycles, for which ΔH° and ΔG° are almost identical,^[7a] the respective differences for the DA reactions are -13.4 [reaction (2)] and -12.6 kcal mol $^{-1}$ [reaction (3)]. These numbers result from the highly positive entropy of the reactions, approximately 45 and 42 entropy units [cal mol $^{-1}$ K $^{-1}$]. This can be understood in terms of flexibility. In the addition of phenanthroline to anthracene, two rigid molecules produce a rigid system. However, owing to the release of the strain, the products of the reaction of **1c** with phenanthroline are “softer” than the starting materials, that is, the bonds have smaller force constants and therefore higher entropies of formation. Thus, the DA reactions are not only enthalpy-driven (strain release) but also entropy-driven, making them far more facile than the corresponding reactions of anthracene.

Generation of 4b and 4c: The generation of **4b** was attempted by the enforced dehydration of **1b** and the thermolysis of **3b**, whereas the generation of **4c** was attempted by the thermolysis of **3c**. The conditions in which **1a** was smoothly dehydrated to **2a** (nitrobenzene, methanesulfonic acid, 130 °C, 20 min) could not be successfully applied to **1b**; no reaction was observed and the starting material remained completely unchanged (by ^1H NMR spectroscopy). If **1b** was treated with the stronger trifluoromethanesulfonic acid, an instantaneous color change of the initial yellow-orange solution to red and finally almost black was observed and its ^1H NMR signals disappeared (Figure 5). At no point were we able to collect evidence (e.g., mass spectrometric) for the intermediary of the dihydrate **2b**. The near-black powder product was insoluble in common organic solvents including chloroform, DCM, THF, toluene, DMF, and methanol. It was therefore analyzed by CP MAS ^{13}C NMR spectroscopy, for which it was necessary to allow the reaction to run for 2 h (instead of minutes) and at 160 °C (instead of 130 °C) to ensure complete conversion.^[13] As can be seen by comparison with the starting material **1b**, the signals of all the saturated (benzylic) carbon atoms disappeared completely, whereas aromatic signals could still be observed (Figure 6) although the shift range of the latter narrowed. This comparison suggests a complete dehydration of the starting cycle, although it is not unequivocal proof (see below). Note, it was not possible to obtain any meaningful mass spectrum of this material. Although the reason for this

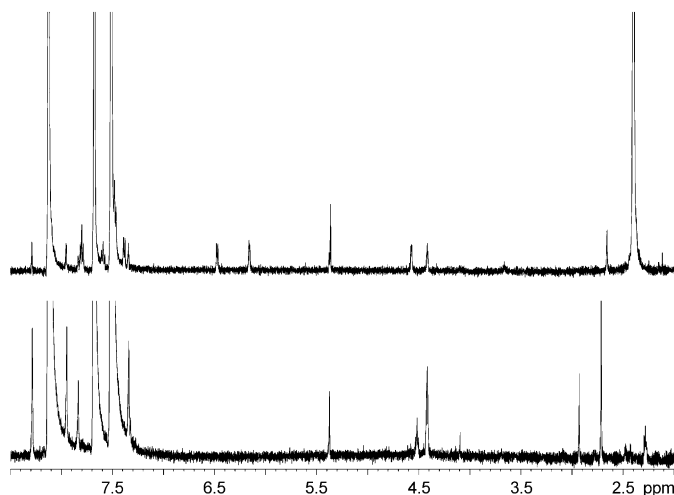


Figure 5. Room-temperature ^1H NMR spectra of a solution of **1b** in $[\text{D}_5]\text{nitrobenzene}$ without acid (top) and after the addition of trifluoromethanesulfonic acid at room temperature and subsequent heating at 100 °C for 8 min (bottom). Note that the signals at approximately $\delta=6.0$ (*exo*-CHO) and 6.5 ppm (*endo*-CHO) and the triplets at $\delta=7.5$ and 7.8 ppm in the top spectrum are absent from the bottom spectrum. The same applies to the signals of **1b** in the aromatic range. The signal at $\delta=4.5$ ppm was not identified.

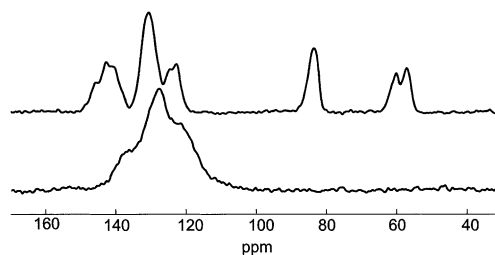


Figure 6. CP MAS ^{13}C NMR spectra of the tetrahydrate **1b** and its dehydration product obtained under enforced conditions.

is unclear, it cannot be excluded that cross-linking took place.

To perform the acetate thermolysis also on the phenyl series, the dihydrate **2b** had to be generated first. However, dihydrates were never observed as intermediates in the above dehydration. To gain access to the key compound **2b**, highly dilute nitrobenzene solutions of **1b** (<0.1 mM) were treated with traces of trifluoromethanesulfonic acid. The crude product of this reaction was analyzed by mass spectrometry and, in fact, the spectrum showed the molecular ion of **2b** at m/z 936. Without isolation, this material was subjected to acetic anhydride/zinc chloride to convert the two ether bridges into four acetate substituents. The product mixture of this conversion was directly subjected to a MALDI-FT mass spectrometric analysis, which gave the spectrum shown in Figure 7. This spectrum not only shows the expected molecular ion of **3b** at m/z 1140, but, most interestingly, also the whole series of acetic acid elimination products of **3b**, including a signal that would fit the molecular ion of the final target **4b** at m/z 900! The signals at m/z

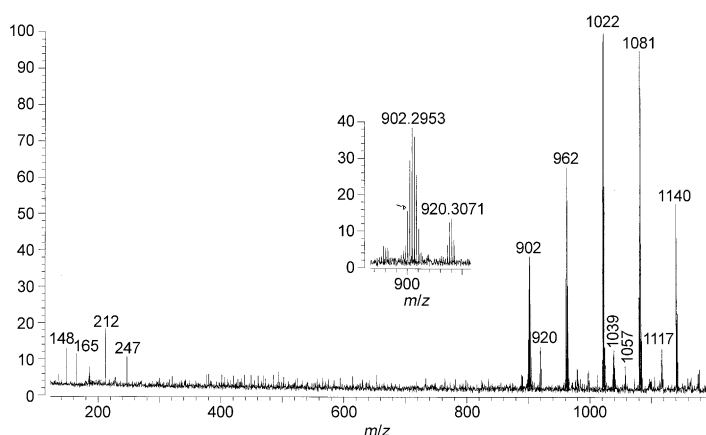


Figure 7. MALDI-FT mass spectrum of the acetylation crude product of **3b** showing the whole sequence of acetic acid elimination reactions starting from the tetraacetate **3b** to the final target "**4b**". The signal groups at m/z 902, 962, and 1022 are accompanied by low intensity signal groups at m/z 920, 980, and 1039, which are a result of the addition of oxygen or "water".

900, 1081, and 1140 were confirmed by high-resolution techniques and established the following formulae: $C_{72}H_{36}$, $C_{78}H_{48}O_6+H$, and $C_{80}H_{52}O_8$, respectively. These formulae represent the target cycle and the triacetate and tetraacetate precursors, respectively. If the same analysis was performed at a higher laser energy, the intensities of the signals due to the precursor molecules decreased whereas that of the target cycle **4b** increased (Figure S1). Clearly, the laser beam affects thermolysis, a phenomenon that is less pronounced within the hexyl series and may point towards a higher tendency of the phenyl-based tetraacetate to suffer elimination of acetic acid than the hexyl-based analogue. MALDI-TOF mass spectrometry with a lower laser energy was also applied. Although the spectra still showed the signal at m/z 900, they looked more complex and thus this technique was not further applied. Note that the molecular ion peaks of the cycles under investigation appear in complex signals groups that are a result of the removal and/or up-take of hydrogen atoms, oxygen atoms, and water molecules. It may therefore be that the most intense signal does not correspond to the molecular ion of the target compound.

After this encouraging finding, we attempted to obtain similar evidence for the unsubstituted parent cycle **4c**. The last fully characterized compound of its synthesis was the open-chain precursor **15** of the tetrahydrate **1c** (Scheme S1). This precursor was cyclized as normal and the crude product mixture of this reaction was analyzed by MALDI-FT mass spectrometry. The full spectrum with an expanded critical range is presented in Figure S2. Despite the use of the crude product, this mass spectrum is relatively simple and exhibits the expected signals for **1c** at m/z 691.1880 and 707.1907 for $[M+Na]^+$ and $[M+K]^+$, respectively, in high resolution. Thus, assuming a cyclic structure, there is no reasonable doubt that the tetrahydrate was contained in the product mixture. The possibility of ring-opening will be addressed

below. Further characterization of this mixture or even isolation of the tetrahydrate **1c** was not attempted because of solubility issues. It was therefore decided to subject this crude product directly to the sequence consisting of 1) methanesulfonic acid catalyzed dehydration to the dihydrate **2c**, 2) tetraacetate generation starting from **2c** to give **3c**, and 3) in situ generation of target **4c** from **3c**. The full spectrum of the product obtained after this sequence is available in Figure 8. As can be seen, the molecular ion of **4c** at m/z 596 is observed, as are the signals of $[M+2H]^+$ and $[M+4H]^+$, known from **4a** and **4b**. In addition, diverse protonation products are observed. All relevant masses were confirmed by high-resolution studies. Thus, the target molecular ion can be obtained for the unsubstituted case!

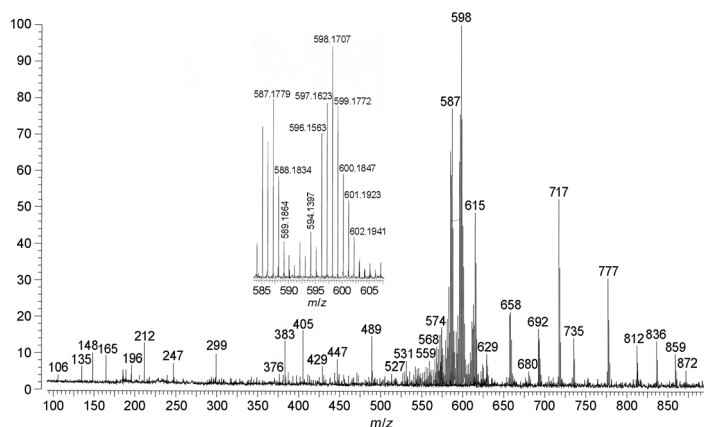


Figure 8. MALDI-FT mass spectrum of the crude product obtained after the reaction sequence from **15** to **4c**. The inset shows the enlarged critical region at high-resolution of the molecular ion of **4c**.

EPR spectroscopic studies of the crude products: As already encountered in previous studies aimed at cycle **II**,^[7a] in this study it was also impossible to obtain reasonable solution NMR spectra of the compounds even though mass spectrometry showed the buckybelt target molecular ion. Apart from solvent signals, the NMR spectra only gave broad lines and those of the aromatic hydrogen atoms even "disappeared" altogether. Figure 9 shows a typical spectrum. The spectra recorded in $[D_5]$ nitrobenzene and $[D_6]$ DMSO at high temperature (100 °C) had the same appearance. Room temperature spectra were not recorded.^[14]

This not only hampered proof of the final structure but also raised concerns as to the possible formation of radicals during thermolysis and dehydration. The crude products obtained from the thermolysis of tetraacetate **3a** and the enforced dehydration of **1b** were therefore investigated by EPR spectroscopy. Figure 10 shows the EPR spectra at room temperature, both with an absorption at $g=2.0026$. This g value indicates a carbon-centered radical that is involved in an extended π -conjugated system.^[15] The formation of a triplet state could be excluded from the shapes and widths of the signals. In particular, there is no zero-field splitting. Although the radical concentrations could not be

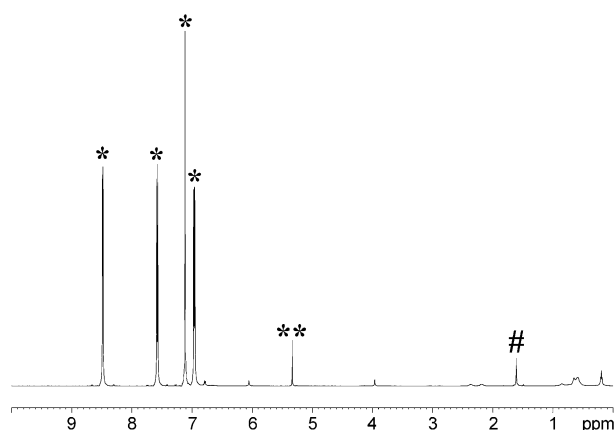


Figure 9. ^1H NMR spectrum of a solution of the thermolysis crude product of **3a** in $[\text{D}_2]$ tetrachloroethane. Although there are a few low intensity signals that could not be assigned, the general appearance of the spectrum is in sharp contrast to the complexity of the mass spectrum obtained from the identical mixture (see Figure 3). Signal assignment: *: phenanthroline, **: solvent, and #: residual acetoxy groups.

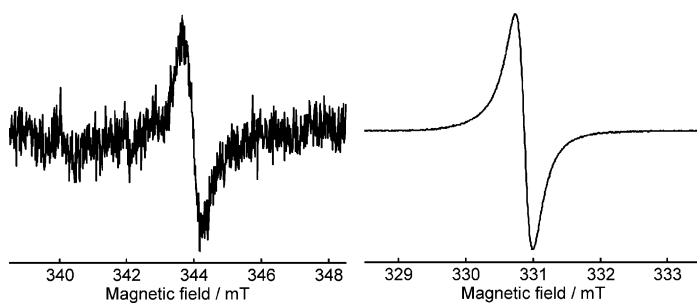


Figure 10. EPR spectra of the thermolysis products obtained from **3a** (left) and **3b** (right).

rigorously quantified, crude estimations based on the mass of the starting material and an external tetramethylpiperidin-1-yloxy (TEMPO) standard suggested trace amounts of radicals in the hexyl case and a few percent in the phenyl case (for details, see the Supporting Information). A temperature-dependent investigation of line intensity revealed a proportionality of signal amplitude to inverse temperature. Such behavior is expected from Curie's law if the concentration of the paramagnetic species is constant. The low concentration suggests that the major fraction of the buckybelts **4a** and **4b** at least are unaffected by radicals. Also, it rules out any eventual disproportionation of the target cycle into a radical cation and a radical anion as a possible mechanism to reduce the strain energy. An equilibrium state of the radical species is ruled out by the constant concentration of the radical. We consider it likely that the EPR signals are caused by an unknown side-product.

Attempted purification revealing the transient nature of thermolysis products: Silica gel TLC separations of the thermolysis (**3a**) and dehydration (**2b**) crude products of the hexyl and phenyl series were performed under ambient con-

ditions and in the absence or presence of oxygen. They always afforded a red spot that moved close to the solvent front for solvents such as chloroform, methylene chloride, or toluene. This spot was followed by an orange band, which in turn was followed by a yellow band. The red spot decolorized both upon standing (under nitrogen) and upon moving further on the plate (under nitrogen). In this process, the red color changed first to orange and then to yellow. If performed under nitrogen, the process took longer. This indicates that the bands following the red spot at the forefront were decomposition products. Several attempts to isolate and analyze any of the colored spots failed altogether. Even attempts in which the silica gel with the red spot was scratched off the TLC plate and analyzed directly by MALDI-FT mass spectrometry did not lead to any conclusive results. Either no signals were observed or the entire collection that had already been obtained from the crude mixture was seen. In line with this disappointing finding, all conventional separations, including column chromatography (using reversed-phase and Buckyrep[®] columns) and recycling gel permeation chromatography (GPC), failed to give single fractions.

Discussion

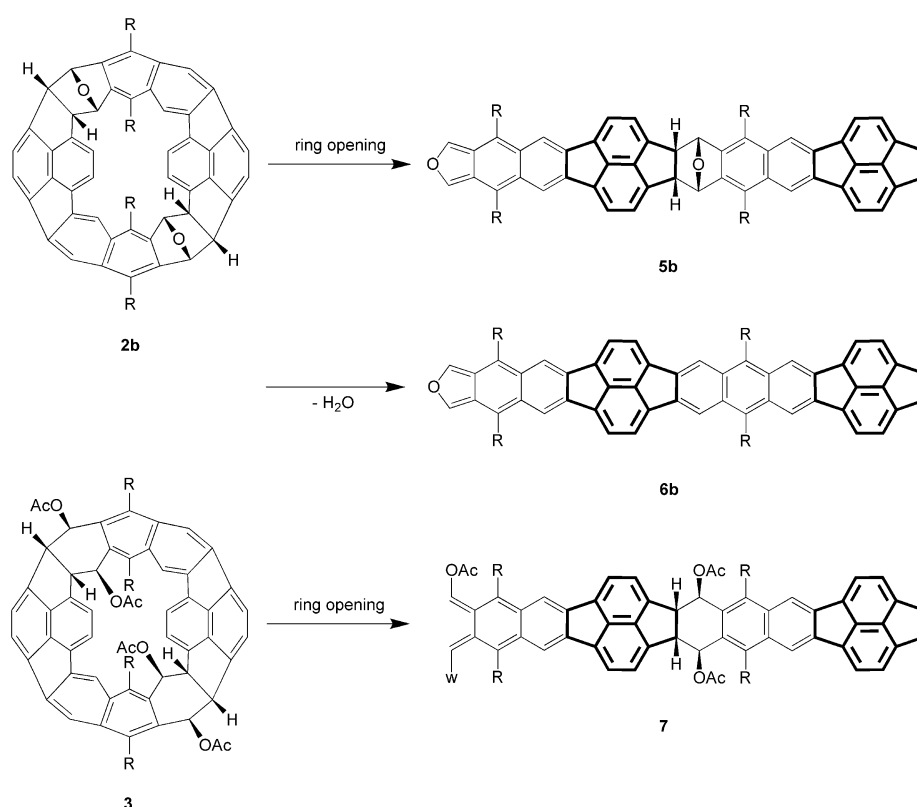
The main motivation behind the work reported herein was to investigate structural alternatives to **4a** that would not be capable of undergoing hydrogen shifts. The work was also encouraged by the hope that the generation of structures **4b** and **4c** would possibly not be accompanied by the formation of radicals, which so effectively prevented an NMR spectroscopic structure proof of **4a**. How far did we get?

The mass spectrometric analysis of the acetylation crude product aiming at **3b** gave the expected molecular ion of **4b** at m/z 900, which is the mass of the fully unsaturated target. In addition, the entire fragmentation cascade, m/z 1140, 1080, 1020, and 960, was detected. These data point to a "well-behaved" mechanism that leads to **4b**. The matching high-resolution mass spectrum of $[M]^+$ at m/z 900.2812 (calcd. 900.2811) removes any lingering doubts regarding the elemental composition of the molecular ion. Despite the rather crude nature of the experiments aimed at the unsubstituted belt **4c**, the fact that for both its precursor **3c** and the belt itself high-resolution mass spectrometric evidence could be obtained suggests that we have found a method to generate compounds of the general structure **4**, at least under mass spectrometric conditions. In contrast to the tetrahexyl congener **4a**, the tetraphenyl belt and the unsubstituted belt have no option to escape their strain by rearrangements involving hydrogen shifts. Rearrangements of the carbon skeleton in the applied temperature range are also unlikely.^[16] The three $[M]^+$ peaks of **4a**, **4b**, and **4c** are therefore considered the first strong evidence for the target belt. Clearly a molecular ion peak, even if highly resolved, does not prove structure. Because of the unfortunate finding that **4b** is somehow associated with seemingly rather persis-

tent radicals (for **4c** this aspect was not investigated), NMR spectroscopic investigations did not lead anywhere. This is the point at which the trapping experiments with the presumed cycle **4a** come in. For a compound with anthracene units one would expect it to be able to undergo DA reactions. As described above, if **4a** was generated in the presence of excess 2,9-dimethyl-1,10-phenanthroline, the mass spectrometric analysis of the crude product mixture showed, in addition to unreacted cycle **4a**, only two groups of adduct signals at m/z 1140 and 1348. The simplest, but not necessarily the only, explanation is that **4a** is trapped once and twice. Again, note that the adducts did not form in the spectrometer but during thermolysis. The reactivity of phenanthrolines as dienophiles is known and the computations clearly show that DA reactions are energetically attractive.^[11]

In addition to these mass spectrometric considerations, the solid-state NMR analysis of the dehydration product of **1b** is of importance. The spectra in Figure 6 prove that the four “water” molecules contained in **1b** can be removed virtually quantitatively. Knowing that **1a** easily dehydrates to **2a**, it is proposed that the dehydration of **1b** to **4b** passes through the same intermediate, namely **2b**.^[17] It is thus tempting to propose that the product spectrum in Figure 6 belongs to **4b**. However, the proposed intermediate **2b** has the potential option to undergo a ring-opening reaction following a (acid-catalyzed) retro-DA path.^[18] Such a path would result in the formation of compound **5b** (Scheme 1), which is unlikely to undergo a subsequent retro-DA reaction because of the already liberated ring strain. Under the applied conditions, compound **5b** would undoubtedly be dehydrated to give **6b**. The existence of **6b**, however, cannot be excluded because both its end groups should have chemical shifts well within the observed range. They would, therefore, be obscured by the signals of the aromatic carbon atoms. Although the mass spectrometric evidence for the retro-DA reaction has no bearing on the behavior of **2b** in acidic solution, such an unwanted reaction cannot be rigorously disproved in the present state of experimentation.

It is worthwhile, in this context, to also have a look at the acetate route and to assess whether open-chain products could possibly be involved. The most likely retro-DA product **7** of any of the tetraacetates **3** is shown in Scheme 1. Although DA addition reactions between 1,4-diacetoxybuta-



Scheme 1. Retro-DA reactions of **2b** and **3** (see text for discussion); a) R = C₆H₁₃, b) Ph, c) H.

dienes and olefins are known, we were not able to find the corresponding retro-reactions. This is in line with mass spectrometric observations; in contrast to all buckybelt di- and tetrahydrates, the tetraacetates **3** do not show any related signals at half mass (for example, see Figure 7). Apart from the question as to whether or not tetraacetate cycles can open up, the most probable initial products of such an opening, compounds **7**, do not have a realistic route for losing the two terminal acetic acids. Such a loss would require a carbene and/or other high-energy intermediary that are unreasonable to propose. It is therefore concluded that the molecular ions for compounds **4** refer, in fact, to cyclic species.

Finally, the UV/Vis spectrum of the fraction of **4a**, which had been analyzed by mass spectrometry and exhibited the pattern m/z 932, 934, and 936,^[7a] is shown in Figure 11.^[19] It has a longest wavelength absorption at approximately $\lambda_{\max} = 550$ nm, which is where one would intuitively expect it on the basis of UV/Vis data for C₆₀ and C₇₀^[20] as well as different C₈₄ isomers^[21] and an open-chain buckyribbon ($\lambda_{\max} = 611$ nm, dichloromethane).^[22] We consider it reasonable that this spectrum is not due to the products of two-fold [1,5]-hydrogen-shifted **4a**.

The synthetic endeavors aimed at fully unsaturated double-stranded cycles have thus reached a rather exciting level. During the last few years different laboratories have got so much closer to the goal than in all the preceding years together. Especially noteworthy is the achievement of

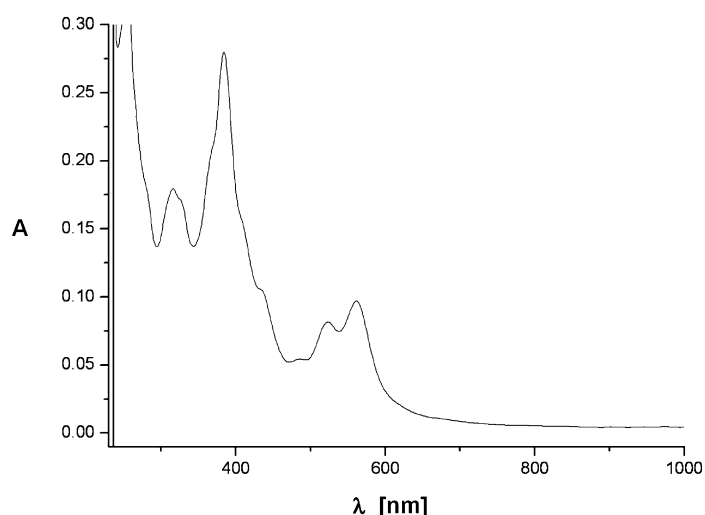
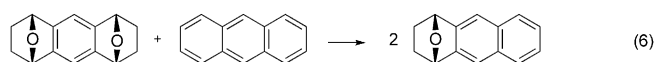
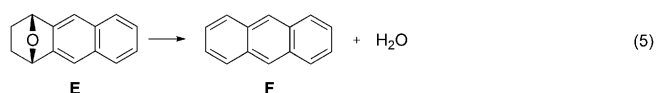
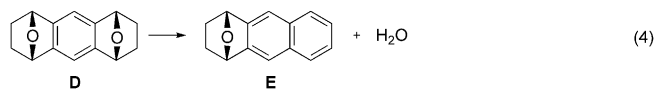


Figure 11. UV/Vis spectrum in chloroform of a GPC fraction obtained from the thermolysis of tetraacetate **3a**.

a conjugated halfcycle with its enormous curvature by Bodwell and co-workers.^[5a] This shows that strong bending of conjugated compounds is not an insurmountable obstacle per se and thus supports the credo of this publication. We have presented circumstantial evidence, each piece of which can be argued, the sum of which, however, proves beyond reasonable doubt that at least for the phenyl- and hydrogen-substituted cases, fully conjugated double-stranded cycles of the general structure **II** have been obtained in the gas phase and may have been obtained in the solution phase. Regarding the latter, the reader is referred to the section below in which theoretical considerations of the dehydration raise questions as to its feasibility. However, substantial effort is still required to find ways to isolate the compounds and ideally grow single crystals for structure analysis.

Theoretical aspects on the sequential elimination of water from 1: Sequential dehydration of **1** leads to systems that contain zero, one, or two **D**-, **E**-, and **F**-like (anthracene) fragments. Thus, as model reactions in nonstrained systems, we studied the dehydration of **D**→**E**→**F** [reactions (4)–(6)] at the G3 and B3LYP/6-311G(d) computational levels. The results, summarized in Table 1, indicate that the B3LYP/6-311G(d) results are less exothermic than the G3 results by an almost constant value of around 2 kcal mol⁻¹ for reactions (4) and (5). However, when a homodesmotic reaction was devised [reaction (6)], this difference is reduced to 0.1–

0.5 kcal mol⁻¹. Thus, it was decided to obtain the thermochemical data for the dehydration reactions of **1**–**3** from homodesmotic/isodesmotic-type equations.



Water is eliminated from **1c** to yield dehydro-**1c** and **D** [reaction (7)]: Two products are possible, dehydro-**1c-1** and dehydro-**1c-2** (Figure 12).

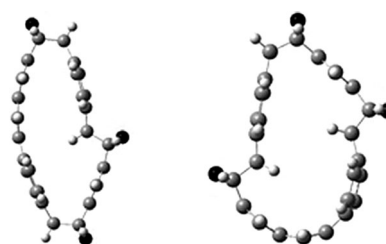


Figure 12. Computed structure of dehydro-**1c-1** (left) and dehydro-**1c-2** (right).

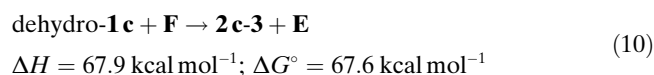
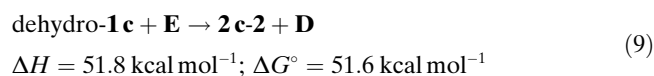
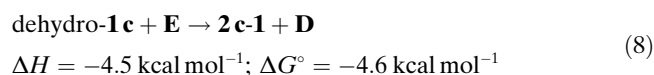
Reaction (7) is exothermic by 4.2 kcal mol⁻¹ when leading to dehydro-**1c-1** and endothermic by 60.3 kcal mol⁻¹ when yielding dehydro-**1c-2**. The free energies for these reactions are similar to the enthalpies of the reactions: -4.9 and +59.5 kcal mol⁻¹, respectively. Because the elimination of water from **D** is exothermic by 19.4 kcal mol⁻¹ [reaction (4)], it can be concluded that the elimination of water from **1c** to yield dehydro-**1c-1** is exothermic by 23.6 kcal mol⁻¹ whereas the elimination to yield dehydro-**1c-2** is endothermic by 40.9 kcal mol⁻¹. The reason for this difference becomes evident when the structures of the two dehydro-**1c** isomers are studied. As was shown in previous studies,^[7] the chemistry of the system is governed by the build-up or release of strain following the reactions. Because only a little strain (or none at all) is released in the transition from **1c** to dehydro-**1c-1** (the structure of **1c** is discussed below), whereas the conjugation gained is larger than in the model reaction, the elimination

Table 1. Results of thermochemical calculations of reactions (4)–(6) at the G3 and B3LYP/6-311G(d) levels of theory.

Reaction	G3			B3LYP		
	$\Delta H(0 \text{ K})$ [kcal mol ⁻¹]	ΔH° [kcal mol ⁻¹]	ΔG° [kcal mol ⁻¹]	$\Delta H(0 \text{ K})$ [kcal mol ⁻¹]	ΔH° [kcal mol ⁻¹]	ΔG° [kcal mol ⁻¹]
4	-21.4	-19.4	-32.2	-19.6	-17.7	-30.1
5	-16.0	-14.0	-26.5	-13.7	-11.8	-24.2
6	-5.4	-5.4	-5.8	-5.9	-5.9	-5.9

has almost the same exothermicity as the elimination of water from **D**. However, due to the large curvature of the aromatic moiety that is formed during the elimination of water to yield dehydro-**1c-2**, this reaction becomes highly endothermic. Clearly, as is also evident from the structure of **2c**, which cannot be formed from dehydro-**1c-2**, the latter is not an intermediate in the reaction that forms **2** from **1** and therefore is not considered further.

Elimination of a second water molecule may lead to three different isomers. This can happen either from the **D**-like moiety or from the **E**-like moiety in dehydro-**1c-1** (hence, dehydro-**1c**). Thus, the elimination reactions of water from dehydro-**1c** to **D** or **E** are represented by the isodesmic reactions (8)–(10). The dehydration of dehydro-**1c** to **2c-1** is more exothermic than the dehydration of **E** by 4.5 kcal mol⁻¹. This means that the absolute exothermicity of this reaction is approximately 24 kcal mol⁻¹, which is in accord with the fact that dehydro-**1c** was never isolated. The first and second water eliminations have similar exothermicities (the second elimination is somewhat more exothermic) and, assuming that the TSs are similar, both occur under the same conditions. The two other possibilities for elimination (leading to **2c-2** and **2c-3**, reactions (9) and (10), respectively) are more endothermic by around 52 and 68 kcal mol⁻¹ relative to **D** and **E**, respectively, which explains why **2c-1** is the only isomer that is isolated from the reaction.



The structures of the products (Figure 13) explain the results on the basis of acquired and released strain. The curvature in **2c-1** is minimal and similar to the curvature in dehy-

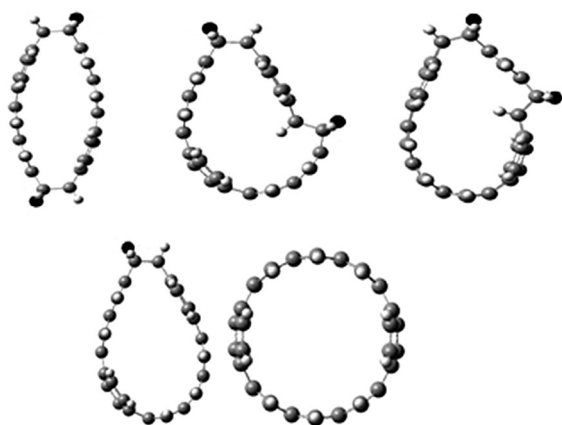
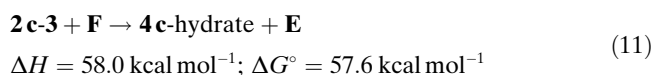


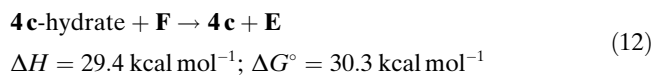
Figure 13. Calculated structures of compounds **2c-1** (top left), **2c-2** (top center), **2c-3** (top right), **4c-hydrate** (bottom left), and **4c** (bottom right).

dro-**1c** such that almost no strain is released or introduced on dehydration and at the same time the conjugation that is gained is greater than in the model compound. However, **2c-2** and **2c-3** are much more curved than dehydro-**1c**, a fact that is manifested by additional strain energy, which causes the overall dehydration reaction to be endothermic.

The third elimination [reaction (11)] is endothermic by 58 kcal mol⁻¹ relative to **E**. This, too, can be explained by the shape of the molecule (Figure 13) because a large degree of curvature is introduced into the structure upon dehydration. The absolute enthalpy of this reaction is approximately +44 kcal mol⁻¹. This result explains the need for a different elimination procedure, as is described in the experimental procedure for **3a**.



The elimination of the last water molecule is endothermic by around 29 kcal mol⁻¹ [reaction (12)] relative to **E** due to the additional strain that is inherent in the resulting structure (Figure 3). Altogether, this renders the process endothermic by 15 kcal mol⁻¹, once again requiring a synthetic route different from simple water elimination.



It is noted that the last elimination is less endothermic than the elimination of the third water molecule [reactions (12) and (11), respectively] and therefore if the elimination from **3** to give **4** was to involve sequential aromatization (i.e., elimination of two HOAc from one ring and only then elimination from the other ring), then the reaction would easily yield **4**. The fact that this does not occur suggests that the process proceeds by elimination of the first two HOAc from different rings and aromatization only occurs in the following steps.

There are several isomers of **1c** that can lead to **2c**. We have considered in the discussion above the experimentally isolated isomer **1c-1**. However, the more symmetric isomer, **1c-2** (Figure 14), in which all the (eliminated) hydrogen atoms are *syn* with respect to the oxygen atoms, was considered as well. The isomer **1c-2** is less stable than **1c-1** by 9.4 kcal mol⁻¹. This can be rationalized by the flatness (thus

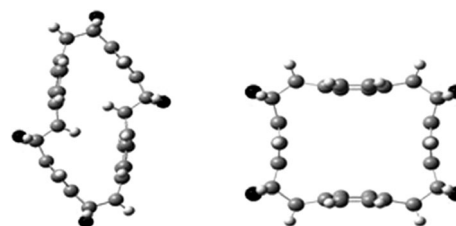


Figure 14. Side-view of **1c-1** (left) and **1c-2** (right).

strainless) naphthalenic moieties in **1c-1**, whereas the same moieties are somewhat curved in **1c-2**. This curvature causes each subunit to be slightly strained (i.e., less than 2.4 kcal mol⁻¹), but this adds up to almost 10 kcal mol⁻¹ for the four naphthalene subunits and probably accounts for the experimental isolation of only **1c-1**.

As mentioned in the results section, **1b** is completely stable under the conditions used for the conversion of **1a** into **2a**. It is rather unlikely that the thermodynamics of the elimination changes dramatically with the substituents (i.e., **a** vs. **b**). However, the kinetics may change due to stabilization or destabilization of reactive intermediates (probably cations, or, less likely but still possible, radicals), which may open up different reaction channels. Under more forceful conditions the elimination proceeded to completion but the product could not be identified. The computational results suggest an endothermicity of 44 kcal mol⁻¹ for this elimination. Assuming a value of ΔS of 30–40 entropy units for the reaction, this means that the elimination of the third water molecule from **2** will have a negative free energy of reaction at temperatures of 830–1190 °C. The calculations were carried out in the gas phase and solvent may change the entropy of the reaction. However, because the reaction was carried out at 160 °C, obtaining the product would suggest that ΔS for the elimination reaction is +102 entropy units, an unreasonable number for such a reaction. Alternatively, if 30–40 entropy units for the elimination are assumed, it implies that the ΔH of the reaction is not larger than around 13–17 kcal mol⁻¹. It is unlikely that the error in the calculations is so large. Therefore, the calculations of the dehydration presented above do not support the formation of **4b** under the forceful elimination conditions. Rather, the option that is described in Scheme 1 (in which **6b** may lose a water molecule in the MS) or a (cationic or radical) polymerization of the cyclic skeleton under these conditions seem to be more reasonable option.

Conclusion

High-resolution mass spectra that match fully conjugated double-stranded cycles **4b** and **4c** were obtained. In contrast with their hexyl-substituted congener **4a**, these two cycles (phenyl-substituted and parent) do not have the option to undergo a [1,5] hydrogen shift that would lead to a disruption of conjugation. It is, therefore, concluded that these intriguing, long-sought-for aromatic belt-type compounds were generated for the first time, at least in the gas phase. Although cycle **4a** could be trapped with phenanthroline, attempts to isolate products **4a–4c** failed.

Experimental Section

The procedures for the synthesis of compounds **1b** and **1c** are described in the Supporting Information. All compounds of the hexyl route have previously been described.^[7a] All reactions involving air-sensitive com-

pounds were carried out under nitrogen using standard Schlenk techniques and dry solvents. All commercial reagents were used without further purification. Solvents were purified and dried by standard procedures.

Analytical methods

Chromatography: Reactions and columns were monitored by thin-layer chromatography (TLC) using TLC silica gel coated aluminium plates 60 UV₂₅₄ (Merck “Kieselgel 60” or Macherey–Nagel with fluorescence indicator F₂₅₄) and visualized by ultraviolet light ($\lambda = 254$ and 366 nm).

NMR spectroscopy: ¹H and ¹³C NMR spectra were recorded on a Bruker AVANCE 300 (¹H: 300 MHz; ¹³C: 75 MHz) or AVANCE 500 (¹H: 500 MHz; ¹³C: 125 MHz) spectrometer at normal probe temperatures using [D]chloroform, 1,1,2,2-[D₂]tetrachloroethane, or [D₅]nitrobenzene. Signals of residual nondeuterated solvent molecules or TMS were used as internal standard for the calibration of the ¹H and ¹³C NMR spectra. Solid-state NMR measurements were performed on a Varian InfinityPlus console using a Chemagnetics 4 mm double-resonance MAS probehead and vortex tube cooling. A standard variable-amplitude cross polarization sequence with XIX proton decoupling (120 kHz rf amplitude) during the acquisition was applied. Saturation pulses were applied before each scan to ensure the same initial condition. A contact time of 2 and 4 ms was chosen. A high-order baseline correction was applied to remove the background signal from the probehead. This was found to be more reliable than a background subtraction. All data were processed by using the matNMR processing toolbox.

Mass spectrometry: High-resolution mass spectra were recorded by the MS service of the Laboratorium für Organische Chemie at ETH Zürich on a Varian IonSpec Ultima MALDI-FT-ICR, a Bruker Daltonics UltraFlex II MALDI-TOF, or a Waters Micromass Autospec Ultima EI-EBE-TriSector instrument. *trans*-2-[3-(4-*tert*-Butylphenyl)-2-methyl-2-propenyldene]malononitrile (DCTB) and 3-hydroxypyridine-2-carboxylic acid (3-HPA) served as matrices for MALDI mass spectrometry.

UV/Vis spectroscopy: UV/Vis spectra were recorded at room temperature on a Perkin–Elmer Lambda 19 instrument using standard 1 cm quartz glass cuvettes.

EPR spectroscopy: The EPR spectra were measured with an ElexSys E680 X-/W-band dual frequency spectrometer (Bruker Biospin GmbH) in X-band mode at typical microwave frequencies of 9.7 GHz. An electron-nuclear double resonator EN 4118X-MD-4 (Bruker Biospin GmbH) was used for both continuous wave (CW) EPR and Mims ENDOR measurements. For CW EPR the resonator was critically coupled, whereas it was overcoupled to $Q \approx 100$ to obtain sufficiently short dead times in Mims ENDOR. For Mims ENDOR a model 250A250A radiofrequency amplifier with a maximum power of 250 W (Amplifier Research, Inc.) was used. Measurement temperatures of 160 K for CW EPR and 80 K for Mims ENDOR were maintained with a CF935 cryostat and ITC 503S temperature controller (Oxford Instruments). Saturation behavior was checked for all samples in CW EPR experiments. An attenuation of 30 dB (microwave power of 0.2 mW) was found to be sufficient to avoid separation. Determination of spin concentration was double checked at 40 dB attenuation (0.02 mW). Glassy frozen solutions of 2,2,6,6-tetramethylpiperidin-1-yloxy (TEMPO) were used as concentration standards and for *g* value reference. Modulation amplitudes of 0.1 or 0.2 mT peak-to-peak were used according to line width. In Mims ENDOR, the pulse lengths were 20 ns for microwave $\pi/2$ pulses and 12 μ s for the radiofrequency pulse, the range from 7–22 MHz was scanned to detect all proton ENDOR signals.

Syntheses

Tetraphenyl-buckybelt (4b): A suspension of the tetraphenyl-buckybelt tetrahydrate **1b** (20 mg, 0.02 mmol) in nitrobenzene (10 mL) was heated to 160 °C. Upon addition of trifluoromethanesulfonic acid (25 μ L, 0.29 mmol) the mixture turned black instantaneously. After 2 h, the solvent and acid were removed by using a rotary evaporator and the residual black material was washed with toluene (5 \times 2 mL) and dried in high vacuum.

CPMAS ¹³C NMR (220 MHz): $\delta = 140$ –110 (peaks at $\delta = 138$, 128, and 120 ppm).

Tetraphenyl-buckybelt dihydrate (2b) and buckybelt dihydrate (2c): A solution of tetrahydrate **1b** (100 mg, 0.10 mmol) or **1c** (80 mg of crude material) in nitrobenzene (**1b**: 1500 mL; **1c**: 50 mL) was heated to 160 °C (**1c**: 140 °C) and treated with trifluoromethanesulfonic acid (**1b**: 20 μ L, 0.23 mmol; **1c**: methanesulfonic acid, 20 μ L, 0.31 mmol) for 2 h (**1c**: 20 min). The solvent was removed by using a rotary evaporator. The residual black solid was washed with toluene (**1b**: 5 \times 10 mL; **1c**: benzene, 5 \times 5 mL) and dried under high vacuum.

2b: MALDI-FT HRMS: calcd. for $[M]^+$: 936.3023; found: 936.3023.

2c: The MALDI-FT mass spectrum did not show any conclusive signals. **Tetraphenyl-buckybelt-tetraacetate (3b) and buckybelt-tetraacetate (3c):** The crude buckybelt-dihydrate **2b** (20 mg) or **2c** (30 mg) were suspended in acetic anhydride (**2b**: 10 mL; **2c**: 5 mL) at 60 °C. A crystal of zinc chloride was added and the reaction mixture was stirred for 6 h (**2c**: overnight) before the solids were filtered off by suction. After washing with ethanol (**2b**: 3 \times 5 mL; **2c**: 5 \times 3 mL), the crude product was dried under high vacuum. Because crude products were used, the amounts of products in mmol cannot be given.

3b: MS (MALDI-FT): m/z : 1140 $[M]^+$, 1080 $[M-60]^+$, 1020 $[M-120]^+$, 960 $[M-180]^+$, 904 $[M-236]^+$, 902 $[M-238]^+$, 900 $[M-240]^+$. HRMS (MALDI-FT): calcd. for $[M]^+$: 1140.3657; found: 1140.3657; calcd. for $[M-AcOH+H]^+$: 1081.3523; found: 1081.3524; calcd. for $[M-4AcOH]^+$: 900.2811; found: 900.2812.

3c: MS (MALDI-FT): m/z : 596 $[M]^+$, 536 $[M-60]^+$, 476 $[M-120]^+$, 416 $[M-180]^+$, 360 $[M-236]^+$, 358 $[M-238]^+$, 356 $[M-240]^+$. HRMS (MALDI-FT): calcd. for $[M-4AcOH]^+$: 596.1565; found: 596.1560.

Computations: The Gaussian 03^[23,24] software package was used for the computations. All the systems underwent full geometry optimization at the B3LYP/6-311G(d) computational level. Frequency (i.e., analytical second derivatives of the energy with respect to $3N-6$ degrees of freedom) calculations were undertaken to verify the energy minima (the number of imaginary frequencies, $N_{\text{imag}}=0$) and to allow thermodynamic calculations. Model systems, namely water, anthracene dihydrate, anthracene hydrate, and anthracene, were also calculated at the G3 level to obtain accurate energy data according to which the B3LYP/6-311G(d) calculations could be calibrated.

Acknowledgements

This work was supported by the Swiss National Funds (SNF 200020-113607 and 200020-126451). We are very thankful to Professor Lawrence T. Scott, Boston College, for sharing with us some of his thoughts on strain effects in aromatic compounds. We thank Dr. M. C. Stuparu for the UV spectrum of **4a** and C. Szabados for help with some of the experiments.

- [1] a) B. D. Steinberg, L. T. Scott, *Angew. Chem.* **2009**, *121*, 5504–5507; *Angew. Chem. Int. Ed.* **2009**, *48*, 5400–5402; b) R. Gleiter, B. Esser, S. C. Kormmeyer, *Acc. Chem. Res.* **2009**, *42*, 1108–1116; c) T. Yao, H. Yu, R. J. Vermeij, G. J. Bodwell, *Pure Appl. Chem.* **2008**, *80*, 533–548; d) K. Tahara, Y. Tobe, *Chem. Rev.* **2006**, *106*, 5274–5290; e) R. Gleiter, B. Hellbach, S. Gath, R. J. Schaller, *Pure Appl. Chem.* **2006**, *78*, 699–706; f) R. Herges in *Modern Cyclophane Chemistry* (Eds.: R. Gleiter, H. Hopf), Wiley-VCH, Weinheim, **2004**, pp. 337–358; g) L. T. Scott, *Angew. Chem.* **2003**, *115*, 4265–4267; *Angew. Chem. Int. Ed.* **2003**, *42*, 4133–4135; h) A. Schröder, H.-B. Meckelburger, F. Vögtle, *Top. Curr. Chem.* **1994**, *172*, 179–201; i) F. H. Kohnke, J. P. Mathias, J. F. Stoddart, *Top. Curr. Chem.* **1993**, *165*, 1–69.
- [2] A. D. Schlüter, *Adv. Mater.* **1991**, *3*, 282–291.
- [3] J. Sakamoto, J. van Heijst, O. Lukin, A. D. Schlüter, *Angew. Chem.* **2009**, *121*, 1048–1089; *Angew. Chem. Int. Ed.* **2009**, *48*, 1030–1069.
- [4] For example, see: F. H. Kohnke, A. M. Z. Slawin, J. F. Stoddart, D. J. Williams, *Angew. Chem.* **1987**, *99*, 941–943; *Angew. Chem. Int. Ed. Engl.* **1987**, *26*, 892–894; F. H. Kohnke, J. F. Stoddart, *Pure Appl. Chem.* **1989**, *61*, 1581–1586.
- [5] a) B. L. Merner, L. N. Dawe, G. J. Bodwell, *Angew. Chem.* **2009**, *121*, 5595–5599; *Angew. Chem. Int. Ed.* **2009**, *48*, 5487–5491. Also, see: b) G. J. Bodwell, J. N. Bridson, M. Cyran'ski, J. W. J. Kennedy, T. M. Krygowski, M. R. Mannion, D. O. Miller, *J. Org. Chem.* **2003**, *68*, 2089–2098; c) G. J. Bodwell, D. O. Miller, R. J. Vermeij, *Org. Lett.* **2001**, *3*, 2093–2096; d) G. J. Bodwell, J. J. Fleming, D. O. Miller, *Tetrahedron* **2001**, *57*, 3577–3585; e) G. J. Bodwell, J. J. Fleming, M. R. Mannion, D. O. Miller, *J. Org. Chem.* **2000**, *65*, 5360–5370; f) G. J. Bodwell, J. N. Bridson, T. J. Houghton, J. W. J. Kennedy, M. R. Mannion, *Chem. Eur. J.* **1999**, *5*, 1823–1827; g) G. J. Bodwell, J. N. Bridson, T. J. Houghton, J. W. J. Kennedy, M. R. Mannion, *Angew. Chem.* **1996**, *108*, 1418–1420; *Angew. Chem. Int. Ed. Engl.* **1996**, *35*, 1320–1321.
- [6] a) Personal communication with M. Iyoda; b) Y. Kuwatani, J.-I. Igarashi, M. Iyoda, *Tetrahedron Lett.* **2004**, *45*, 359–362; c) T. Yoshida, Y. Kuwatani, K. Hara, M. Yoshida, H. Matsuyama, M. Iyoda, S. Nagase, *Tetrahedron Lett.* **2001**, *42*, 53–56; d) Y. Kuwatani, T. Yoshida, K. Hara, M. Yoshida, H. Matsuyama, M. Iyoda, *Org. Lett.* **2000**, *2*, 4017–4020.
- [7] a) C. Denekamp, A. Etinger, W. Amrein, A. Stanger, M. Stuparu, A. D. Schlüter, *Chem. Eur. J.* **2008**, *14*, 1628–1637; b) M. Stuparu, V. Gramlich, A. Stanger, A. D. Schlüter, *J. Org. Chem.* **2007**, *72*, 424–430; c) M. Stuparu, D. Lentz, H. Rüegger, A. D. Schlüter, *Eur. J. Org. Chem.* **2007**, 88–100; d) W. D. Neudorff, D. Lentz, M. Anibarro, A. D. Schlüter, *Chem. Eur. J.* **2003**, *9*, 2745–2757.
- [8] a) J. E. Norton, B. H. Northrop, C. Nuckolls, K. N. Houk, *Org. Lett.* **2006**, *8*, 4915–4918; b) E. Clar, J. W. Wright, *Nature* **1949**, *163*, 921–922; c) E. Clar, *Chem. Ber.* **1949**, *82*, 495–514.
- [9] Malte Standera, PhD Thesis, ETH Zurich (Switzerland), **2010**.
- [10] Whether there are phenanthroline adducts derived from a reaction with the compound with m/z 936 cannot be decided because of signal complexity. If the perception is correct (see ref. [7a]), that the signals at m/z 934 and 936 are due to the addition of two and four hydrogen atoms to the 9,10-positions of the one and two anthracenes of **4a**, respectively, the compound with m/z 936 would not have an appropriate site to undergo a Diels–Alder reaction.
- [11] For phenanthrolines as dienophiles see the work presented at the third Brisbane biological and organic chemistry symposium: D. Margetic, R. N. Warrener, D. N. Butler, 1,3-Dipolar Cycloadditions to Polycyclic Aromatic Hydrocarbons, the Queensland University of Technology, Brisbane, **2002**.
- [12] A. Koshio, M. Inakuma, T. Sugai, H. Shinohara, *J. Am. Chem. Soc.* **2000**, *122*, 398–399.
- [13] The material obtained under milder conditions still contained residual water molecules.
- [14] R. H. Mitchell, R. V. Williams, T. W. Dingle, *J. Am. Chem. Soc.* **1982**, *104*, 2560–2571.
- [15] F. Gerson, W. Huber *Electronspin Resonance Spectroscopy of Organic Radicals*, Wiley-VCH, Weinheim, **2003**.
- [16] A. J. Stone, D. J. Wales, *Chem. Phys. Lett.* **1986**, *128*, 501–503. It cannot be excluded that Stone–Wales rearrangements take place under mass spectrometric conditions. They would lead to different structures than the proposed ones here, but would not affect double-strandedness.
- [17] For **2b** a high-resolution mass spectrum shows $[M]^+$ at m/z 936.3023 (calcd: 936.3023).
- [18] Note that as for **2a**, the mass spectra of **2b** and **2c** also show signals due to retro-DA products. For the latter they appear as $[M/2+Na]^+$ and $[M/2+K]^+$.
- [19] M. Stuparu, PhD Thesis, ETH Zurich (Switzerland), **2007**.
- [20] H. Ajie, M. M. Alvarez, S. J. Anz, R. D. Beck, F. Diederich, K. Fostiropoulos, R. Huffman, W. Krätschmer, Y. Rubin, K. E. Schriver, D. Sensharma, R. L. Whetten, *J. Phys. Chem.* **1990**, *94*, 8630–8633.
- [21] J. Crassous, J. Rivera, N. S. Fender, L. Shu, L. Echegoyen, C. Thilgen, A. Herrmann, F. Diederich, *Angew. Chem.* **1999**, *111*, 1716–1721; *Angew. Chem. Int. Ed.* **1999**, *38*, 1613–1617.

- [22] B. Schlicke, A. D. Schlüter, P. Hauser, J. Heinze, *Angew. Chem.* **1997**, *109*, 2091–2093; *Angew. Chem. Int. Ed. Engl.* **1997**, *36*, 1996–1998.
- [23] Gaussian 03 Revision D.02, M. J. Frisch, G. W. Trucks, H. B. Schlegel, G. E. Scuseria, M. A. Robb, J. R. Cheeseman, J. A. Montgomery, Jr., T. Vreven, K. N. Kudin, J. C. Burant, J. M. Millam, S. S. Iyengar, J. Tomasi, V. Barone, B. Mennucci, M. Cossi, G. Scalmani, N. Rega, G. A. Petersson, H. Nakatsuji, M. Hada, M. Ehara, K. Toyota, R. Fukuda, J. Hasegawa, M. Ishida, T. Nakajima, Y. Honda, O. Kitao, H. Nakai, M. Klene, X. Li, J. E. Knox, H. P. Hratchian, J. B. Cross, V. Bakken, C. Adamo, J. Jaramillo, R. Gomperts, R. E. Stratmann, O. Yazyev, A. J. Austin, R. Cammi, C. Pomelli, J. W. Ochterski, P. Y. Ayala, K. Morokuma, G. A. Voth, P. Salvador, J. J. Dannenberg, V. G. Zakrzewski, S. Dapprich, A. D. Daniels, M. C. Strain, O. Farkas, D. K. Malick, A. D. Rabuck, K. Raghavachari, J. B. Foresman, J. V. Ortiz, Q. Cui, A. G. Baboul, S. Clifford, J. Cioslowski, B. B. Stefanov, G. Liu, A. Liashenko, P. Piskorz, I. Komaromi, R. L. Martin, D. J. Fox, T. Keith, M. A. Al-Laham, C. Y. Peng, A. Nanayakkara, M. Challacombe, P. M. W. Gill, B. Johnson, W. Chen, M. W. Wong, C. Gonzalez, J. A. Pople, Gaussian, Inc., Wallingford CT, **2004**.
- [24] L. A. Curtiss, K. Raghavachari, P. C. Redfern, V. Rassolov, J. A. Pople, *J. Chem. Phys.* **1998**, *109*, 7764–7776.

Received: February 9, 2011

Revised: May 13, 2011

Published online: September 14, 2011